Surface-Based Observations of Volcanic Emissions to the Stratosphere

Dave Hofmann[1], John Barnes[1], Ellsworth Dutton[1], Terry Deshler[2],
Horst Jäger[3], Richard Keen[4], and Mary Osborn[5]

Long-term, surface-based observations of the stratospheric aerosol layer are presented and compared. These include three LIDAR aerosol backscatter measurements, at Mauna Loa Observatory (Hawaii), Langley Research Center (Virginia), and Garmisch-Partenkirchen (Germany); balloonborne in situ particle concentration measurements at Laramie, Wyoming, solar visible transmission measurements at Mauna Loa Observatory; aerosol optical depth measurements at South Pole Station and Mauna Loa Observatory; and lunar eclipse optical depth determinations, which is a globally integrating technique. Surface-based measurements have provided a useful historical record of volcanic effects on the stratospheric aerosol and the agreement between the various techniques is very good. However, some uncertainties exist when the stratosphere is relatively free of volcanic aerosol and some of the techniques are not able to easily resolve the very small amount of aerosol from natural and/or anthropogenic sources. The lunar eclipse data, which go back to the late 1800s, suggest that the Pinatubo eruption in 1991 probably perturbed the stratospheric aerosol layer at least as much as that of Krakatau in 1883. This is an important observation as it is one of the few ways to accurately compare the stratospheric effects of eruptions prior to modern measurements that began in the late 1950s. At the time of this writing (September 2002) the stratosphere appears to be at background with the lowest level of aerosol observed since the layer was discovered in 1959.

[1]Climate Monitoring & Diagnostics Laboratory, NOAA, Boulder, Colorado
[2]University of Wyoming, Laramie, Wyoming
[3]Forschungszentrum Karlsruhe, IMK-IFU, Garmisch-Partenkirchen, Germany
[4]University of Colorado, Boulder, Colorado
[5]Langley Research Center (SAIC), NASA, Hampton, Virginia

Volcanism and the Earth's Atmosphere
Geophysical Monograph 139

10.1029/139GM04

1. INTRODUCTION

Enhanced twilights following major volcanic eruptions have been the historical indicators of the sudden injection of particulate matter into the stratosphere. Thus parameters such as the "Dust Veil Index" [*Lamb*, 1970, 1977], to gauge the severity of the atmospheric effects of eruptions, came into existence. In situ measurements of the nature of stratospheric particulate material in the late 1950s by *Junge et al.* [1961] revealed that sulfur was the main particle composition. They postulated that the source of this "sulfate layer," during a period when the stratospheric aerosol content was very low due to a dearth of volcanic injections for the previous 25 years, was sulfurous gases of Earthly origin. Thus, the stratospheric particle layer is often referred to as the "Junge Layer." There is also a small micro-meteoritic com-

ponent of the background aerosol related to the ablation of meteors in the stratosphere. However, the episodic injection into the stratosphere of material from major volcanic eruptions is the main source of stratospheric aerosol. The importance of the aerosol layer becomes obvious following these eruptions as an initial stratospheric heating, due to radiation absorption by the aerosol, followed by a global tropospheric cooling, related to aerosol backscatter of solar radiation, results [*Hansen et al.*, 1978; *Dutton and Christy*, 1992]. In addition, the added surface area of the volcanic aerosol particles enhances heterogeneous chemical reactions which affect stratospheric ozone [*Solomon*, 1999].

Utilizing particle vaporization techniques with balloonborne particle counters, *Rosen* [1971] showed that the stratospheric particles consisted of a solution having an approximately 75% sulfuric acid, 25% water composition, or a "stratospheric sulfuric acid aerosol" as it became known. Following the eruption of Fuego (Guatemala) in 1974, *Hofmann and Rosen*, [1977] used balloonborne optical particle counters to show that particles from the eruption were also made up of this sulfuric acid-water mixture and that only a very small fraction was in the form of nonvolatile material, i.e., silicate or other crustal material. Condensation nuclei detectors flown on balloons after the Mt. St. Helens (Washington state, USA) eruption in 1980 [*Hofmann and Rosen*, 1982] showed that new sulfuric acid aerosol was formed from the gas phase following the eruption. It was thus postulated that the main, lasting effect on the stratosphere was volcanic injection of sulfur dioxide which chemically converted to sulfuric acid vapor followed by condensation into sulfuric acid droplets. The "dust" or "ash" particles, being of larger size, apparently fall out of the stratosphere within a few months during the early eruption decay phase. Further study of the chemical conversion both theoretically [*McKeen et al*., 1984] and from satellite data [*Bluth et al.,* 1992] indicate that the characteristic time of conversion of sulfur dioxide into sulfuric acid vapor is about 1 month. Growth of new and pre-existing droplets by vapor accretion follows, increasing droplet size and total mass by an order of magnitude or more. The sulfuric acid-water aerosol which forms, decays with an e-folding time of about 1 year.

It has now been over 30 years since more or less continuous measurements of the stratospheric aerosol layer began from surface-based sites. In what follows we review some of the longer records obtained by laser radar (LIDAR), balloonborne optical particle counters, solar atmospheric transmission measurements, solar optical depth and lunar eclipse optical depth. We apologize for not being able to include all records that may exist but chose those that have the longest continuous records and are readily available.

2. LIDAR OBSERVATIONS

The first application of a "ruby optical maser," later to become LIDAR, an acronym for "LIght Detection And Ranging," to particle detection was made by *Smullin and Fiocco* [1962]. The "particle" was the Moon and optical echoes of 50 joule pulses of 694 nm ruby laser radiation were detected at Lexington, Massachusetts, in May of 1962. Following the eruption of the volcano Agung on Bali in 1963, *Grams and Fiocco* [1967] applied an "optical radar" (pulsed ruby laser) to detect backscatter from volcanic particles in the stratosphere. This was the forerunner of many LIDAR measurement programs operating today, three of the longest records being those from Garmisch-Partenkirchen (GAP), Germany (47.5°N) which began in 1976; Langley (LRC), Virginia (37.1°N); and Mauna Loa Observatory (MLO), Hawaii (19.5°N) both of which began in 1974.

Method

The ground-based atmospheric aerosol LIDAR systems included in this paper employ either a ruby or Nd:YAG pulsed laser transmitter and an optical receiver in parallel or collinear arrangement. The system transmits intense, short duration light pulses of linear polarization at a high repetition rate into the receiver field of view. The intensity of the light elastically backscattered by atmospheric molecules and particles is measured versus time, or equivalently altitude, through the telescope receiver, collimating optics, and an appropriate detector. The signal profile is stored by a fast analog-to-digital converter or by a photon counting device. Relative intensity data are accumulated separately from all altitude intervals for a selected averaging period, which may include thousands of individual laser shots.

This provides a high-resolution vertical profile of the optical scattering characteristics of aerosols, clouds, and the background molecular atmosphere. Typically the profiles obtained from many laser shots are averaged together to reduce noise. Raw data products are profiles of total backscatter, i.e., molecular plus particle backscatter signals. The particle backscatter signal must be separated from the molecular signal by suitable algorithms. Primary data products are then profiles of aerosol backscatter or scattering ratio. Secondary products are aerosol extinction profiles and aerosol optical depth.

The LIDAR scattering ratio, a primary parameter derived from the analysis of LIDAR data, is defined as

$$R(z) = \frac{b_a(z) + b_m(z)}{b_m(z)} \quad (1)$$

where b_a (z) is the aerosol backscatter and b_m (z) is the molecular backscatter, both in units of 1/(km-sr) and both at altitude z. The molecular backscatter is calculated from a temperature-pressure profile obtained by a nearby radiosonde launch, just prior to or just after the LIDAR data are collected. The scattering ratio is calculated by evaluating

$$R(z) = \frac{CS(z)z^2}{b_m(z)T^2(z)} \quad (2)$$

where S (z) is the LIDAR signal received from altitude z, T^2 (z) is the two-way atmospheric transmittance, and C is a system constant determined by normalizing the right-hand side of the equation to an expected minimum value of R over a specified altitude range. The transmittance is calculated from a combination of radiosonde-derived molecular extinction model or LIDAR-derived aerosol extinction, and model ozone absorption. During periods of moderate to heavy aerosol loading, aerosol extinction must be scaled to the aerosol backscatter using a model extinction-to-backscatter ratio [*Jäger and Hofmann*, 1991]. The LIDAR equation (2) is then solved several times using an updated value of aerosol extinction for each iteration.

The integrated stratospheric aerosol backscatter is defined as

$$\int_{h_t}^{30km} b_a(z)dz \quad (3)$$

where h_t is the height of the tropopause. b_a (z) can be easily obtained from $R(z)$ and b_m (z) using equation (1). Integrated aerosol backscatter is a good measure of the stratospheric column loading, and can be converted to optical depth using an appropriate extinction-to-backscatter ratio.

Results

All three LIDAR records investigated here began with ruby lasers as used by *Grams and Fiocco* [1967] in the early work. However, as the ruby lasers aged and advances in laser technology made high pulse repetition rate, multiple wavelength lasers available, two of the three ruby lasers (GAP and MLO) were replaced in the 1990s with Nd:YAG lasers which have a primary wavelength of 1064 nm and a double-frequency wavelength of 532 nm. Because of its ease of detection, the latter wavelength has become a standard for stratospheric aerosol work.

To extend the ruby record at GAP and MLO, the backscatter at the ruby wavelength (694 nm) was calculated from the measured backscatter of the Nd:YAG laser. At GAP, the 532 nm laser measured backscatter was used along with a model of the wavelength dependence of aerosol backscatter using balloonborne aerosol size distribution measurements [*Jäger and Hofmann*, 1991; *Jäger et al.*, 1995, *Jäger and Deshler*, 2002]. At MLO, both the 532 nm and the 1064 nm backscatter were measured and the value at 694 nm was determined by simple interpolation. In the latter case, an overlap period of the ruby and Nd:YAG lasers indicated that the interpolation technique produced a similar result as the ruby LIDAR itself, in fact, due to the higher repetition rate of the Nd:YAG laser (30 Hz as compared to 0.1 Hz), the statistics of the latter were considerably better.

A distinct advantage of LIDAR measurements is the ability to obtain a vertical profile of aerosol backscatter. In this sense they provide additional information compared to column measurements such as optical depth and solar transmission. In Plate 1 we compare vertical profiles of the LIDAR backscatter ratio at three locations during a period of high volcanic aerosol loading (July 1992, about a year after the eruption of Pinatubo) and a background period (June-July, 1999). In situ measurements of particle mixing ratio (particles per milligram of air) from Laramie, Wyoming, for the same periods are also shown.

The time history of integrated backscatter coefficient from three LIDARs is compared in Plate 2. The integral in all cases includes the entire stratosphere. Although the agreement between the three LIDARs is generally good, there are several noticable differences. The onset of the El Chichón and Pinatubo events at MLO is more abrupt. This is related to the fact that both were low-latitude eruptions and the volcanic aerosol enhancement was observed more promptly at the lower latitude MLO site than at the other two midlatitude sites. The early decay phases, especially after the Pinatubo eruption, also occur more promptly at MLO, possibly for the same reasons. While MLO indicates a uniform annual variation after about 1996, which has been interpreted as indicating the background, non-volcanic level of stratospheric aerosol [*Barnes and Hofmann*, 2001], the midlatitude sites suggest a continuing decline although the measurement statistics are not very good at these sites after about 1999.

Vertical profiles of scattering ratio at 694 nm from three LIDARs during the background period (July 1999) are compared in Plate 3. The stratospheric aerosol layer resides at higher altitudes (lower air densities) at lower latitudes because of the increase in tropopause height from pole to equator. The increase in altitude of the aerosol layer will in turn increase the scattering ratio, which is scaled to air den-

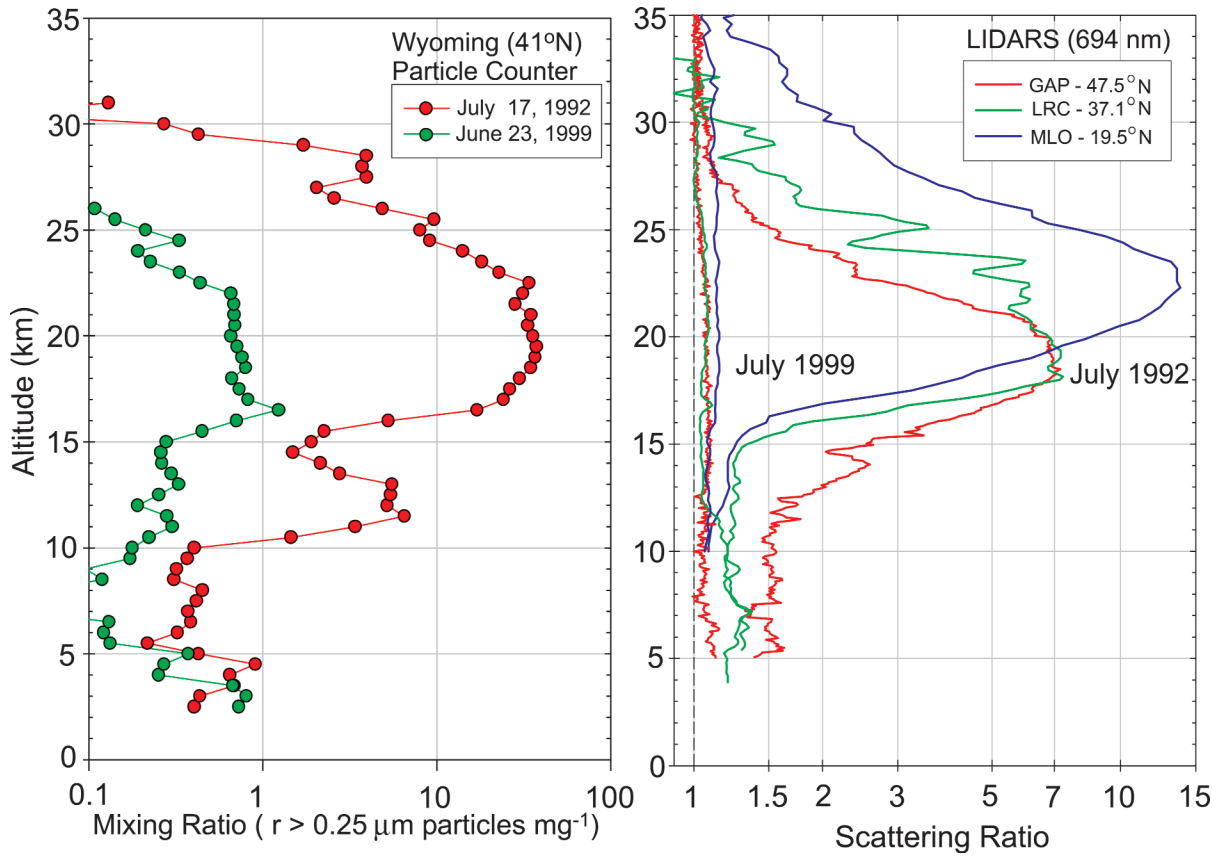

Plate 1. Vertical profiles of particle mixing ratio (particles per mg of air) for aerosol particles having radii greater than 0.25µm (left panel) using balloonborne optical particle counters at Laramie, Wyoming, and of lidar scattering ratio, (aerosol + molecular)/molecular, at 694 nm (right panel), from three lidars at Garmisch-Partenkirchen, Germany (GAP), Langley Research Center, Virginia (LRC), and Mauna Loa Observatory, Hawaii (MLO). Data are shown for two periods, June–July 1992 (about 1 year after the eruption of Pinatubo) and during a volcanically quiescent period, June–July 1999. An enlarged version of the 1999 lidar profiles is given in Plate 3.

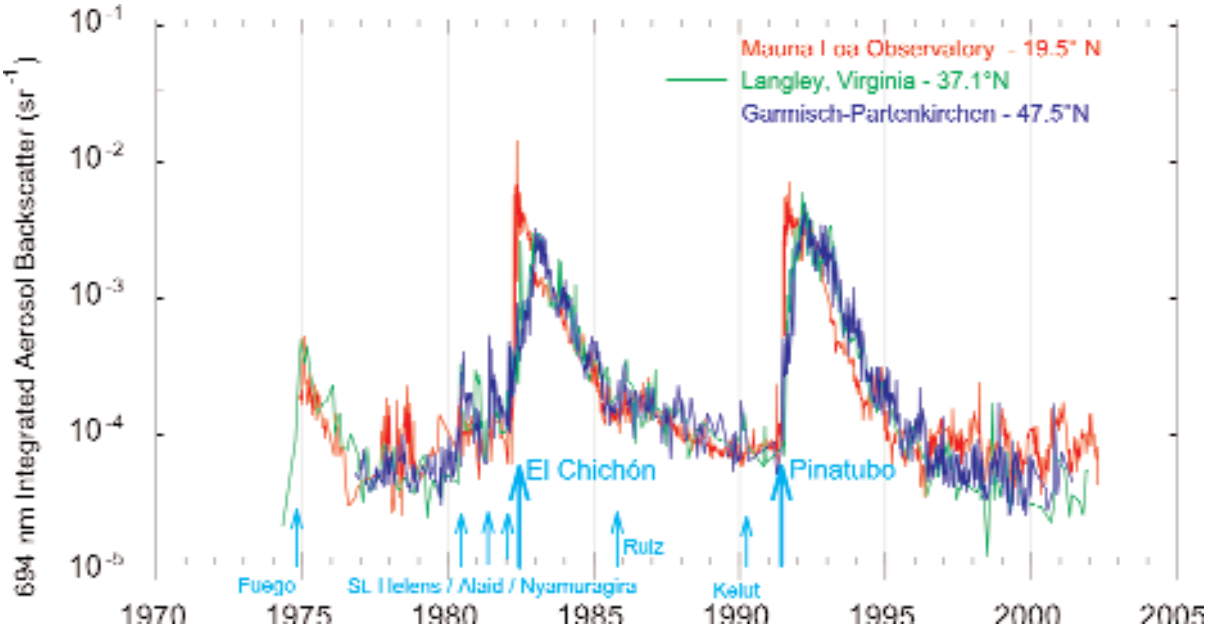

Plate 2. Aerosol backscatter integrated throughout the stratosphere at the 694 nm ruby wavelength at three sites where long-term records are available versus time since the 1970s. The arrows and names indicate the occurrences of volcanic eruptions that are known to have perturbed the stratospheric aerosol layer.

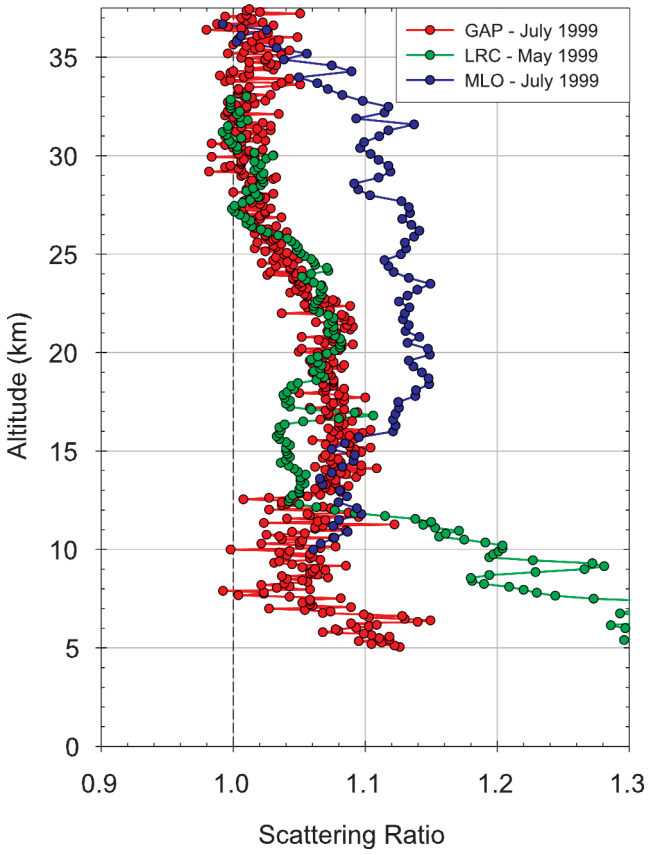

Plate 3. LIDAR scattering ratio profiles at Garmisch-Partenkirchen, Germany (GAP) at 47.5°N, Langley Research Center, Virginia (LRC) at 37.1°N, and Mauna Loa Observatory, Hawaii (MLO) at 19.5°N, during the volcanically quiescent period during the summer of 1999. The data are for the 694 nm wavelength with the GAP and MLO data determined from the 532 nm Nd:YAG laser data.

sity through the dependence on molecular backscatter, for the same total aerosol scatter, i.e., scattering ratio is an atmospheric mixing ratio. This is clearly observed in the MLO measurements.

The data in Plate 2 suggest that the peak aerosol effects on the stratosphere after the El Chichón and Pinatubo eruptions were of similar magnitude, yet it was observed by satellite that Pinatubo injected about three times as much sulfur dioxide [about 20 megatons—*Bluth et al.*, 1992] as El Chichón. This is related to the fact that the initial El Chichón eruption cloud came directly from Mexico to the Hawaiian Islands and caused the largest integrated backscatter ever observed (see the narrow spike in Plate 2 with an integrated backscattering coefficient of about 1.2×10^{-2} sr^{-1}, 200 times the pre-eruption level.) In general, measurements from a few discrete sites are not adequate to judge the relative intensity of eruptions prior to a time when more or less global uniformity in the stratospheric aerosol distribution has been achieved.

The rate of sulfuric acid aerosol droplet growth following an equatorial eruption depends, among other factors, on the density of the reacting/condensing sulfurous gases in the equatorial reservoir. The latter is a region equator-ward of about 20° [*Grant et al.*, 1996]. Some factors that affect the density of sulfuric acid that can form, in addition to the amount of sulfur dioxide injected, is the rate of oxidation of the parent volcanic gas, which can be reduced if the reactant hydroxyl radical concentration is depleted by excessive sulfur dioxide, thus causing self-limiting growth [*Pinto et al.*, 1989]. The sulfuric acid growth rate also depends on the altitude of the injection through aerosol size-dependent growth variations [*Hamill et al.*, 1977]. Another factor that can affect growth through reducing the gas density is dispersion related to transport to higher latitudes [*Hofmann*, 1987]. Meridional transport from the equatorial region occurs primarily in winter and is enhanced with westerly stratospheric winds. Since transport depends on season, aerosol particle size will depend to some degree on the season of the eruption and the phase of the quasi-biennial oscillation (QBO) in the direction of stratospheric equatorial winds.

The eruption of El Chichón (17.4°N, April 4, 1982) occurred in the southern hemisphere fall and that of Pinatubo (15.1°N, June 15, 1991) in the southern hemisphere winter. Both occurred during the easterly phase of the QBO, but the vertical wind structure was different with strong easterlies above 21 km for El Chichón, but above 25 km for Pinatubo. Since easterlies generally inhibit poleward dispersal of equatorial stratospheric air toward the winter hemisphere, the sulfurous gases from El Chichón were initially confined to the equatorial region and northern hemisphere compared to Pinatubo when large transport of material into the southern hemisphere was observed [*Trepte et al.*, 1993]. The El Chichón eruption occurred two months earlier than Pinatubo, and thus before southern hemisphere winter. This suggests that considerably more particle growth could occur prior to transport out of the equatorial reservoir region for El Chichón, while transport south and possibly the self-limiting affect of large amounts of sulfur dioxide, probably resulted in less relative growth for Pinatubo, even though more sulfur dioxide was injected. Satellite data show the large increase in aerosol extinction following the Pinatubo eruption in the southern hemisphere early in the event [*McCormick and Veiga*, 1992], and the optical depth data at the south pole (to be shown later) showed the Pinatubo event to be much larger than the El Chichón event at this remote site. MLO is situated near the equatorial reservoir northern boundary and likely did not sample the Pinatubo aerosol at its most concentrated state as it apparently did for El Chichón.

Relatively minor aerosol backscatter increases were observed after the eruptions of Mt. St. Helens, Alaid and Ruiz, in 1980, 1981 and 1986, respectively. In addition, the eruption of Nyamuragira early in 1982, caused an observable stratospheric aerosol increase just prior to the major eruption of El Chichón. These eruptions were either too weak (e.g., Alaid, Ruiz, Nyamuragira, Kelut) or contained too little sulfur (e.g., Mt. St. Helens) to cause significant perturbations to the stratospheric aerosol. The high latitude of some of these eruptions (e.g., Alaid, Mt. St. Helens) also limits their global impact.

3. BALLOONBORNE PARTICLE COUNTERS

One of the longest records of stratospheric aerosol measurement has been produced by the University of Wyoming's balloonborne optical particle counter program. Approximately monthly in situ measurements of the vertical profile of stratospheric aerosol size distributions and number concentrations have been maintained since 1971. Several different particle counters have been utilized but two size ranges have been preserved throughout the period, particles having radii greater than 0.15 μm and greater than 0.25 μm [*Deshler et al.*, 2003]. These data will be presented here and compared with other techniques, in particular LIDAR instruments which also give vertical profile information.

Method

The University of Wyoming optical particle counter, initially developed by *Rosen* [1964], is a white light counter

measuring aerosol scattering in the forward direction and using Mie theory to determine aerosol size. Light scattered from particles passing through the light beam is collected over a 30° half-angle cone and focused onto a photomultiplier tube for pulse height discrimination. Two symmetrical independent photon paths are used to limit noise, and the influence of cosmic rays in the stratosphere, by coincidence counting. These instruments are sensitive to optically detectable aerosol as small as 0.15 μm in radius. Initial observations in the 1970s consisted of measurements of particles ≥ 0.15 and 0.25 μm at a sample flow rate of 1 liter min^{-1}. Current measurement capabilities consist of condensation nuclei (r > 0.01 μm) and optically detectable aerosol, r ≥ 0.15–2.0 μm in twelve size ranges at a flow rate of 10 liters min^{-1} [*Deshler et al.*, 2003]. These instruments are flown on balloons to obtain aerosol profiles from the surface to altitudes of over 30 km.

Results

The particle concentrations in two size ranges, as measured in balloon flights at Laramie, Wyoming, since 1971, have been integrated between altitudes of 15 and 25 km and are shown in Plate 4. All major volcanic eruptions, which occurred during this period, show up clearly in the record. As in the LIDAR record, the magnitude of the El Chichón and Pinatubo events are similar for reasons discussed earlier. The value of the optical particle counter data is in their size-selective properties which indicate that the size distribution is dominated by larger particles after a major volcanic eruption. This is related to the excessive growth of sulfuric acid droplets at this time. The in situ data at Laramie indicate that the stratospheric aerosol at northern mid latitudes likely reached a minimum in 1997–1998 at a value similar to that in 1979 and 1990 for the smaller particle size range (r ≥ 0.15 μm) but slightly lower for the larger particle size range (r ≥ 0.25 μm). On a mass basis, this would suggest that the stratosphere is probably in its cleanest state since at least about 1959 when the sulfate layer was discovered by *Junge* [1961] following a long volcanically quiescent period. This would also agree with the midlatitude LIDAR data at LRC and GAP, the LIDAR backscatter being closely related to the mass present in the stratosphere [*Hofmann and Barnes*, 2002].

In Plate 5 we compare the LIDAR and balloon data which confirm that the LIDAR backscatter variations follow those of the larger particle size range closely.

4. SOLAR VISIBLE TRANSMISSION

Accurate measurements of the broadband solar transmission of the atmosphere from a clean, high altitude site is a relatively inexpensive way to monitor aerosol levels in the stratosphere. The apparent transmission technique was first used at Mauna Loa Observatory by *Ellis and Pueschel* [1971] and showed that there were no significant trends related to air pollution for the 1958–1970 period. These data have been extended and reported by *Dutton and Bodhaine* [2001] and are updated here.

Method

The apparent transmission method uses ratios of the total direct solar irradiance measured at different fixed solar elevation angles during the course of a clear morning or afternoon. A daily average of three such ratios is taken as the day's apparent transmission, which is insensitive to instrument calibration uncertainties due to the cancellation of the linear instrument calibration factor in the ratio. It has been shown that variations in the apparent transmission are due primarily to aerosols whereas water vapor sensitivity is muted due to line saturation. Monthly averages of apparent transmission have been used to reduce some local variability and develop a long time series of the MLO apparent transmission. For further explanation of the apparent transmission method and past analysis of the record see *Dutton and Bodhaine* [2001] and references therein.

Results

The broadband visible solar radiation transmission data at MLO as measured since 1958, are shown in Plate 6. Most notable are the decreases in transmission associated with major volcanic eruptions that occurred during this period. They include Agung in 1963, Fuego in 1974, El Chichón in 1982, and Pinatubo in 1991. Here also the El Chichón eruption caused a large initial spike that decayed rapidly in 1982. Perhaps a better comparison of the severity of the El Chichón and Pinatubo eruptions as observed at MLO would be the area under the transmission curves in Plate 6. Springtime pollution events, related to the long-range transport of Asian desert dust, have been observed at Mauna Loa Observatory for many years [*Bodhaine et al*., 1981]. These events are clearly observed in the Mauna Loa solar transmission record in Plate 6.

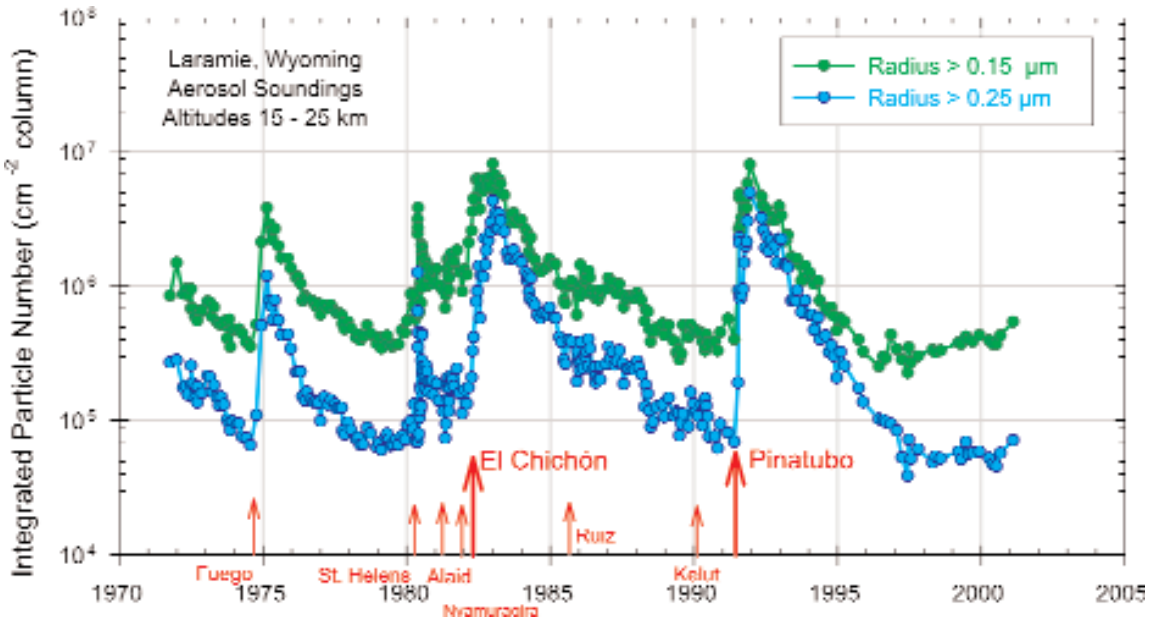

Plate 4. Stratospheric aerosol particle column abundances between 15 and 25 km for two size ranges as measured in individual balloon flights at Laramie, Wyoming (41°N) since 1971. The occurrence of volcanic eruptions that affected the stratospheric aerosol level are indicated in red. Vertical profiles of the aerosol particle mixing ratio for June 1992 and July 1999 were given for the r > 0.25 µm size range in Plate 2.

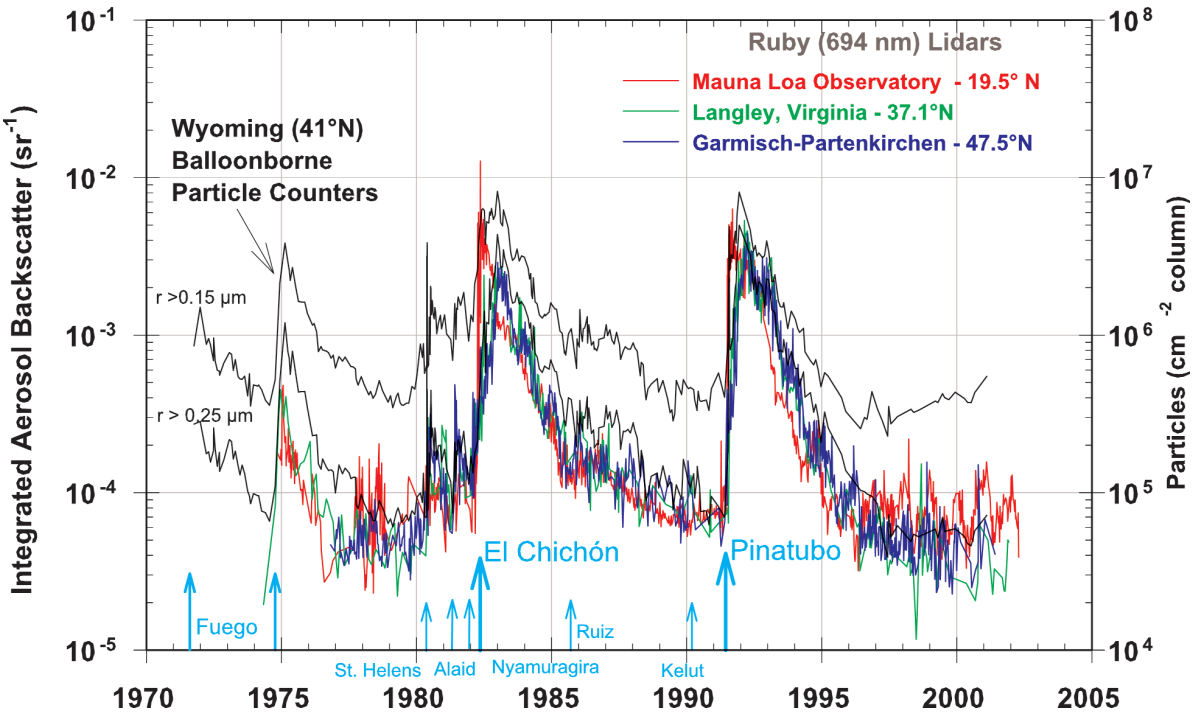

Plate 5. Comparison of LIDAR integrated backscatter and optical particle counter column integrated data showing that the LIDAR data generally agrees better, in terms of time variations, with the larger particle size range (r > 0.25 µm) than the smaller sized particles.

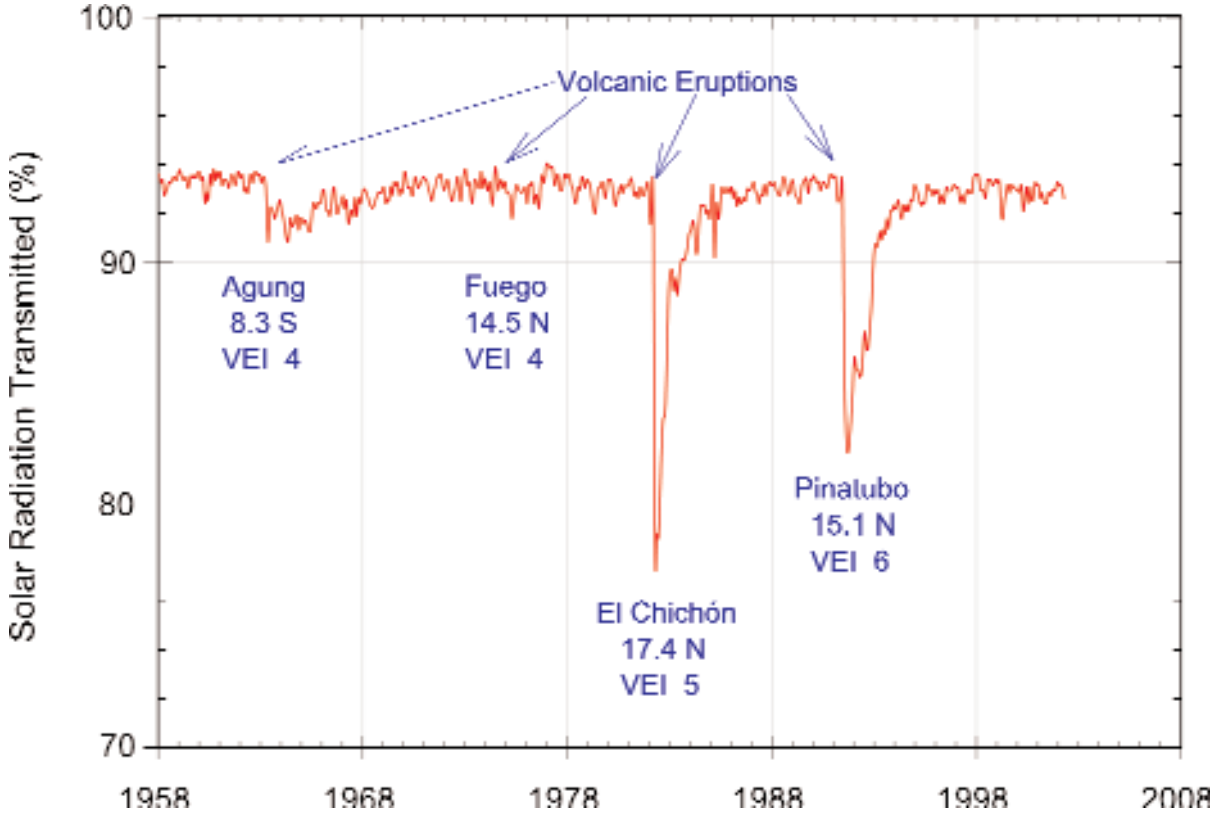

Plate 6. Transmission of solar radiation through the clean Mauna Loa Observatory atmosphere at an elevation of 3.4 km as determined since 1958. The names, latitudes and volcanic explosive index of eruptions that perturbed the stratosphere during this period are indicated in the Plate. The light blue line is the estimated transmission for an aerosol-free atmosphere. The small annual decreases in transmission are real and are associated with enhanced springtime transport of Asian effluents to the site.

5. AEROSOL OPTICAL DEPTH

The aerosol optical depth or thickness (τ) of the atmosphere is defined as the negative of the natural logarithm of the ratio of intensity of direct solar radiation of a particular wavelength at the top of the atmosphere to that at the surface, and is thus an absolute measure of the transmission of the atmosphere. The average value of τ at solar visible wavelengths for a volcanically unperturbed stratospheric aerosol is about 0.02, which includes the upper troposphere. The maximum value that has been observed following major volcanic eruptions is about 0.3, or a reduction of the direct solar intensity by about 25%.

There have been a number of attempts to establish global stratospheric aerosol optical depth climatologies [*Sato et al.,* 1993; *Stothers*, 1996]. Varying techniques used to estimate optical depth after volcanic eruptions range, for example, from early dust veil indices to pyrheliometry to satellite measurements of aerosol extinction. Because the data quality has increased over time, the uncertainties in the records decline with time as well. However, these analyses provide useful databases for the history of volcanic eruptions which perturbed the stratosphere and thus for long-term climate simulations.

Method

Aerosol optical depths at NOAA Climate Monitoring and Diagnostics Laboratory observatories have been deduced under clear skies over the past three decades using a low accuracy but relatively stable method of comparing wideband filtered (Schott glass) pyrheliometer measurements to simple spectral radiative transfer calculations. Progressively larger aerosol optical depths are introduced into the model until the best agreement with the observations is achieved. While the absolute accuracy of the resulting optical depth when compared to modern sunphotometer measurements is on the order of 0.04 optical depth units, the long-term precision of the measurements appears to be close to 0.01, which rivals the best results achieved to date from sunphotometers. Some previous results of these observations at the four main CMDL observatories are given by *Dutton and Christy* [1992].

Results

Aerosol optical depth observations at the U.S. South Pole Station in Antarctica were chosen for this analysis because it is remote from the sites of the eruptions and is relatively free of obscuring tropospheric aerosol. In Plate 7 these data are compared to aerosol optical depth measurements using the same technique at Mauna Loa Observatory to place the overall observations in perspective. Since the sun cannot be observed at the south pole in winter, the South Pole Station record has breaks in it. The large optical depth at Mauna Loa immediately after the El Chichón eruption is again related to the transport of the Mexican eruption cloud directly over the Hawaiian Islands early in the event. At south pole, Pinatubo caused a larger optical depth than El Chichón; however, the El Chichón peak was expected in southern winter 1983 when the sun was not present for observations. The Pinatubo event as observed at the south pole would be expected to be much larger than the El Chichón event, both because more sulfur dioxide was involved in the Pinatubo event and because the initial transport was to the south, arriving in summer rather than in winter as was the case for El Chichón.

It is interesting to note the springtime minima in the south pole optical depth record that occurred each year following the Pinatubo eruption. These minima are believed to be related to the large-scale subsidence that occurs within the antarctic vortex during winter and to the fallout from the stratosphere of ice crystals and nitric acid hydrate particles (polar stratospheric cloud particles) that form around sulfuric acid droplets in the austral winter resulting in the now familiar drying and denitrification of the antarctic winter stratosphere. These processes are prerequisites for the springtime ozone hole chemistry to take place when the sun appears.

6. LUNAR ECLIPSE OPTICAL DEPTH

About once per year, on average, the Moon is eclipsed as it passes into the Earth's shadow; at these times the Moon is visible due to sunlight refracted (and to a much lesser extent, scattered) into the shadow by the Earth's atmosphere. *Kepler* [1604] attributed the near disappearance of the Moon during an eclipse in 1588 to "mists and smoke" in the atmosphere, and the volcanic nature of these atmospheric aerosols became apparent when a dark eclipse followed the 1883 eruption of Krakatau [*Flammarion*, 1884]. Comparing *Link's* [1956] theory with photometric observations of three eclipses following the 1963 eruption of Agung, *Hansen and Matsuhima* [1966] derived quantitative values for aerosol optical depth. Thus, our satellite can be used as a remote sensor of the globally averaged optical depth of stratospheric aerosols of volcanic origin.

Conceptually, the linkage between volcanic aerosols and lunar eclipses is as follows. Most of the refracted sunlight that illuminates the eclipsed Moon passes through the stratosphere. Stratospheric aerosols reduce the transmission

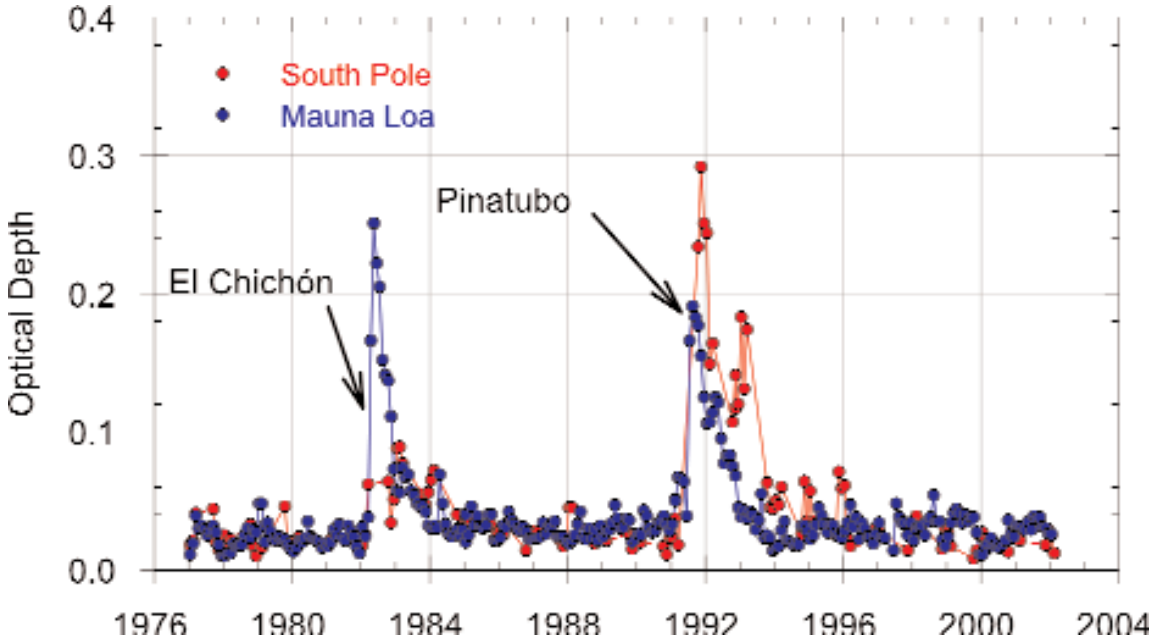

Plate 7. Aerosol optical depth measured with pyrheliometers at South Pole Station and Mauna Loa Observatory.

of sunlight into the umbra. The path length of sunlight through a stratospheric aerosol layer is about 40 times the vertical thickness of the layer (this factor is for a layer concentrated between heights of 15 and 20 kilometers, but the factor can range between 25 and 50 for other layer heights and depths and various eclipse geometries). Therefore, the brightness of the eclipsed Moon is extremely sensitive to the amount of aerosols in the stratosphere.

Method

Aerosol optical depths can be calculated for the date of an eclipse from the difference between the observed brightness of the eclipse and a modeled brightness computed for an aerosol-free standard atmosphere, modified by assumed distributions of ozone and cloud. Details of this technique, applied to observations during 1960 through 1982, appear in *Keen* [1983]. Using this technique, optical depths have been derived from observations of all 38 total lunar eclipses between 1960 and 2001. In addition, results from all eight total eclipses during the period 1880-1888 have been included to allow comparison with the effects of the Krakatau eruption in 1883. In all, six distinct increases, believed to be associated with volcanic eruptions, were identified in the derived optical depth data. The probable identities of the eruptions are given in Table 1.

During any total lunar eclipse, the Moon is illuminated by sunlight passing through every latitudinal segment of the Earth's limb; hence, the brightness of the Moon is affected by volcanic aerosols at all latitudes, and the derived optical depths may be considered a global average. This interpretation is particularly true for those eclipses (about one-third of all total lunar eclipses) for which the Moon's disk passes across the center of the Earth's shadow. However, during some eclipses, the Moon may pass north or south of the Earth's shadow axis, and the derived optical thickness is weighted toward aerosols in the respective hemisphere of the Earth. This sampling bias was particularly apparent during the first year or so following the eruptions of Agung and El Chichón, when higher concentrations of aerosols occurred in the southern and northern hemisphere, respectively, and eclipses crossing the same (or opposite) hemisphere produced systematically higher (or lower) optical depths (relative to an exponential decay curve). An empirical correction factor of 0.8 removed most of these systematic differences (if the Moon passed south of the Earth's shadow axis during an eclipse following Agung, the derived optical thickness was multiplied by 0.8, while the derived value was divided by 0.8 if the Moon passed north of the axis). As indicated later, the derived optical depth following major eruptions is of the order 0.1 ±0.01. Since the empirical correction factor of 0.8 is derived from these observations, the uncertainty in the factor is of the same relative magnitude, i.e., ±0.1. The correction factor was applied to the optical depths following the eruptions of Agung, Fuego, and El Chichón. Although the Pinatubo eruption occurred in

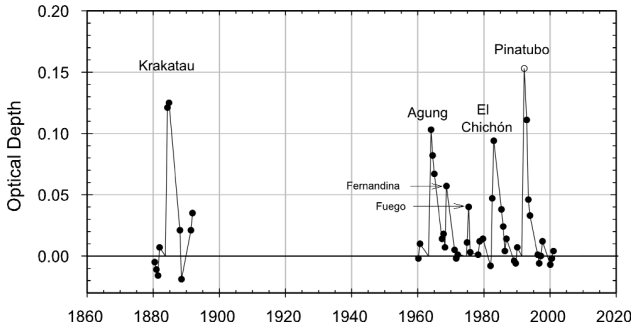

Figure 1. Optical depth following major volcanic eruptions as determined by the lunar eclipse technique for the periods 1880-1888 and 1960-2000. Zero points prior to the eruptions of Krakatau, Agung, Fuego, and Pinatubo are estimated. The peak value following the Pinatubo eruption (open circle in graph) is estimated (see text).

Table 1. Volcanic Eruption Data and Lunar Eclipse Derived Maximum Optical Depth

Volcano Name	Latitude	Longitude	Major Eruption Date	Volcanic Explosive Index[a]	Maximum Optical Depth
Krakatau	6.10ºS	105.43ºE	1883-08-27	6	0.13
Agung	8.34ºS	115.51ºE	1963-03-17	4	0.10
Fernandina	0.37ºS	91.55ºW	1968-06-11	4	0.06
Fuego	14.47ºN	90.88ºW	1974-10-10	4	0.04
El Chichón	17.36ºN	93.23ºW	1982-04-03	5	0.09
Pinatubo	15.13ºN	120.35ºW	1991-05-15	6	0.15

[a]*Simkin and Siebert* [1994]

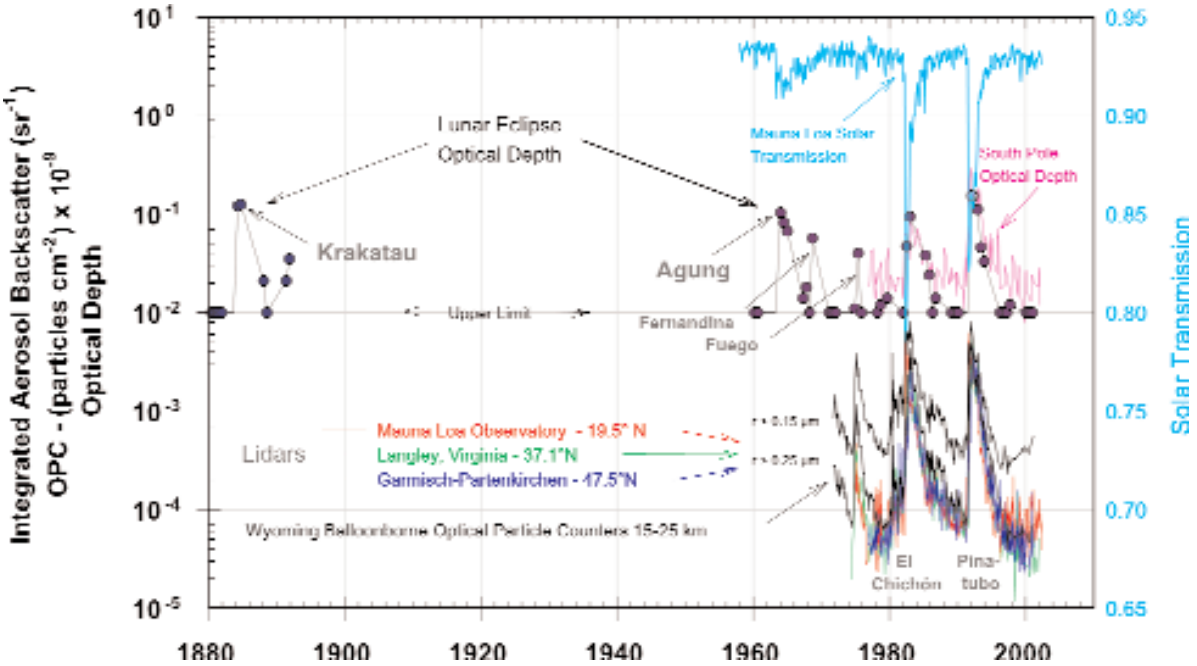

Plate 8. Summary of long-term stratospheric aerosol records including three lidars, at Mauna Loa Observatory (Hawaii), Langley Research Center (Virginia), and Garmisch-Partenkirchen (Germany); balloonborne particle counters at Laramie, Wyoming, solar visible transmission at Mauna Loa Observatory; aerosol optical depth at South Pole Station; and lunar eclipse optical depth, which is a globally-integrating technique.

the northern hemisphere, it was near the meteorological equator at the time of the eruption, so no corrections were applied. The four eclipses following the Krakatau eruption were all central eclipses (the Moon crossed the Earth's shadow axis), so no corrections were applied to that event.

Optical depths were set to zero on the dates of the eruptions of Krakatau, Agung, Fuego, and Pinatubo; observed values were near zero for eclipses close to the dates of the eruptions of Fernandina and El Chichón. No lunar eclipses occurred until 18 months following the Pinatubo eruption in June 1991, while results from Agung and El Chichón indicate that peak optical depths occurred about 9 months after those eruptions. Therefore, the time series of optical depths following Pinatubo was extrapolated backwards to a date 9 months after the eruption using a composite decay curve (with a time constant of 1.92 years) derived from the Agung and El Chichón eclipse data.

Results

Of the 46 eclipses for which optical depths were derived, 15 have elevated values apparently due to volcanic eruptions. The mean optical depth derived from the other 31 eclipses is 0.002, with a standard deviation of 0.009. This indicates that the probable error of each derived optical depth is about ±0.01. Occurrences of maximum global optical depths substantially larger than 0.01 are listed in Table 1 with probable volcanic eruption identification. The identification of Fernandina with the 1968 peak is uncertain. Increases of observed values to slightly above the 0.01 uncertainty level occurred in 1979 and in late 1997. If real, these slightly elevated values could indicate aerosols from the eruptions of Soufriere on St. Vincent (1979) and Soufriere Hills on Montserrat (1997). All optical depth determinations are plotted in Figure 1.

Maximum observed values of 0.13 for Krakatau occurred for eclipses 8 and 14 months after the eruption, and the actual maximum could be slightly greater. For Pinatubo, the maximum value of 0.15 is extrapolated from an observed value of 0.11 for an eclipse 18 months after the eruption. Furthermore, if the aerosol layer height for either event was higher than the 15 to 20 kilometer height assumed for these calculations, the optical depth could be as much as 30% greater. It is, therefore, within the range of error that the two events produced approximately the same maximum optical depth.

7. SUMMARY AND CONCLUSIONS

Plate 8 compares most of the long-term records presented here. We conclude that the agreement is remarkable, in particular, between the optical depth measurements at the south pole and by the lunar eclipse technique following the El Chichón and Pinatubo eruptions.

Because of its global stratospheric integrating properties, the lunar eclipse technique is perhaps the most definitive for defining the global effect of volcanic eruptions on the stratospheric aerosol. The results suggest that not only did the Pinatubo eruption have a larger effect on the stratosphere than the El Chichón event, but that it is likely that it was at least as large as the Krakatau event. At this time, lunar eclipses which occurred after other volcanic events between the period 1888 and 1960 have not been analyzed. This period includes about 30 eruptions which had Volcanic Explosive Indices (VEI) of 4 or greater, including three with VEI's of 5 and two with 6 [*Simkin and Siebert*, 1994]. Included in the latter is the 1902 eruption of Santa Maria (14.75ºN) in Guatemala which, occurring at low latitude, likely had a global effect on the stratosphere. In addition, observations for most eclipses exist back to about 1800. Completing this unique record of the effects of volcanic eruptions on the global stratosphere over a 200-year period is a goal worth pursuing.

REFERENCES

Barnes, J. E., and D. J. Hofmann, Variability in the stratospheric background aerosol over Mauna Loa Observatory, *Geophys. Res. Lett., 28*, 2895-2898, 2001.

Bodhaine, B. A., B. G. Mendonca, J. M. Harris, and J. M. Miller, Seasonal variations in aerosols and atmospheric transmission at Mauna Loa Observatory, *J. Geophys. Res., 86*, 7395-7398, 1981.

Bluth, G. J. S., S. D. Doiron, C. S. Schnetzler, A. J. Krueger, and L. S. Walter, Global tracking of the SO_2 clouds from the June 1991 Mount Pinatubo eruptions, *Geophys. Res. Lett., 19*, 151-154, 1992.

Deshler, T. M., E. Hervig, C. Kröger, D. J. Hofmann, J. M. Rosen, and J. B. Liley, Thirty years of in situ stratospheric aerosol size distribution measurements from Laramie, Wyoming (41°N), using balloonborne instruments, *J. Geophys. Res.,108,* 4167.doi:10.1029/2002JD002514, 2003.

Dutton, E. G., and B. A. Bodhaine, Solar irradiance anomalies caused by clear-sky transmission variations above Mauna Loa: 1958-1999, *J. Climate, 14*, 3255-3262, 2001.

Dutton, E. G., and J. R. Christy, Solar radiative forcing at selected locations and evidence for global lower tropospheric cooling following the eruptions of El Chichón and Pinatubo, *Geophys. Res. Lett., 19*, 2313-2316, 1992.

Ellis H. T., and R. F. Pueschel, Solar radiation: Absence of air pollution trends at Mauna Loa, *Science, 172*, 845-846, 1971.

Flammarion, C., L'eclipse totale de lune du 4 Octobre, *L'Astronomie 3*, 401- 408, 1884.

Grams, G., and G. Fiocco, Stratospheric aerosol layer during 1964 and 1965, *J. Geophys. Res., 14*, 3523-3542, 1967.

Grant, W. B., E. V. Browell, C. S. Long, L. L. Stowe, R. G. Grainger, and A. Lambert, Use of volcanic aerosols to study the tropical stratospheric reservoir, *J. Geophys. Res*., *101*, 3973-3988, 1996.

Hamill, P., O. B. Toon, and C. S. Kiang, Microphysical processes affecting stratospheric aerosol particles, *J. Atmos. Sci., 34*, 1104-1119, 1977.

Hansen, J. E., and S. Matsushima, Light illuminance and color in the Earth's shadow, *J. Geophys. Res. 71*, 1073-1081, 1966.

Hansen, J. E., W.–C. Wang, and A. A. Lacis, Mount Agung eruption provides test of a global climatic perturbation, *Science, 199*, 1065-1068, 1978.

Hofmann, D. J., Perturbations to the global atmosphere associated with the El Chichón volcanic eruption of 1982, *Rev. Geophys., 25*, 743-759, 1987.

Hofmann, D. J., and J. E. Barnes, Interannual variability in the background stratospheric aerosol over Mauna Loa Observatory and the effects of the quasi-biennial oscillation, *Network for the Detection of Stratospheric Change 2001 Symposium*, Archachon, France, 24-27 Sept., p. 131, 2002.

Hofmann, D. J., and J. M. Rosen, Balloon observations of the time development of the stratospheric aerosol event of 1974-75, *J. Geophys. Res., 82,* 1435, 1977.

Hofmann, D. J., and J. M. Rosen, Balloonborne observations of stratospheric aerosol and condensation nuclei during the year following the Mt. St. Helens eruption, *J. Geophys. Res., 87*, 11,039-11, 061, 1982.

Jäger, H., and T. Deshler, Lidar backscatter to extinction mass and area conversions for stratospheric aerosols based on midlatitude balloonborne size distribution measurements, *Geophys.Res. Lett*., *29*, doi:10.1029/2002GL015609, 2002.

Jäger, H., and D. Hofmann, Midlatitude lidar backscatter to mass, area, and extinction conversion model based on in situ aerosol measurements from 1980 to 1987, *Appl. Opt., 30*, 127-138, 1991.

Jäger, H., T. Deshler, and D. J. Hofmann, Midlatitude lidar backscatter conversions based on balloonborne aerosol measurements, *Geophys. Res. Lett., 22*, 1729-1732, 1995.

Junge, C. E., C. W. Chagnon, and J. E. Manson, Stratospheric aerosols, *J. Meteorol., 18*, 81-108, 1961.

Keen, R., Volcanic aerosols and lunar eclipses, *Science, 222*, 1011-1013, 1983.

Kepler, J., *Astronomiae Pars Optica*, Marnium and Aubrii, Frankfurt, pp. 267-284, 1604.

Lamb, H. H., Volcanic dust in the atmosphere, with a chronology and assessment of its meteorological significance, *Phil. Trans. Royal Soc. London, Series A, 266*, 425-533, 1970.

Lamb. H. H., Supplemental dust veil index assessments, *Climate Monitor, 6*, 57-67, 1977.

Link, F., *Die Mondfinsternisse*, Akademische Verlagsgesel-lschaft, Leipzig, 127 pp., 1956.

McCormick, M. P., and R. E. Veiga, SAGE II measurements of early Pinatubo aerosols, *Geophys. Res. Lett., 19*, 155-158, 1992.

McKeen, S. A., S. C. Liu, and C. S. Kiang, On the chemistry of stratospheric SO_2 from volcanic eruptions, *J. Geophys. Res., 92*, 4873-4881, 1984.

Pinto, J. P., R. P. Turco, and O. B. Toon, Self-limiting physical and chemical effects in volcanic eruption clouds, *J. Geophys. Res., 94*, 11,165-11,174, 1989.

Rosen, J. M., The vertical distribution of dust to 30 km, *J. Geophys. Res., 69,* 4673-4676, 1964.

Rosen, J. M., The boiling point of stratospheric aerosols, *J. Appl. Meteorol*. 10, 1044, 1971.

Sato, M., J. E. Hansen, M. P. McCormick, and J. B. Pollack, Stratospheric aerosol optical depths, 1850-1990, *J. Geophys. Res., 98*, 22,987-22,994, 1993.

Simkin, T., and L. Siebert, *Volcanoes of the World*, 349 pp., Geoscience Press, Inc., Tucson, 1994.

Smullin, L. D., and G. Fiocco, Optical echoes from the Moon, *Nature, 194*, 1267, 1962.

Solomon, S., Stratospheric ozone depletion: A review of concepts and theory, *Rev. Geophys*., *37*, 275-316, 1999.

Stothers. R. B., Major optical perturbations to the stratosphere from volcanic eruptions: Pyrheliometric period, 1881-1960, *J. Geophys. Res., 101*, 3901-3920, 1996.

Trepte, C. R., R. E. Veiga, and M. P. McCormick, The poleward dispersal of Mount Pinatubo volcanic aerosol, *J. Geophys. Res., 98,* 18,563-18,573, 1993.

J. Barnes, Mauna Loa Observatory, Rm. 202, NOAA, P.O. Box 275, Hilo, HI 96721

T. Deshler, Dept. of Atmospheric Science, University of Wyoming, Laramie, Wyoming 82071

E. Dutton and D. Hofmann, Climate Monitoring and Diagnostics Laboratory, NOAA, 325 Broadway, Boulder, CO 80305-3328

H. Jäger, Forschungszentrum Karlsruhe, IMK-IFU, Kruezechbahnstr. 19, 8100 Garmisch-Partenkirchen, Germany

R. Keen, PAOS-UCB 311, University of Colorado, Boulder, CO 80309

M. Osborn, Code 475, NASA Langley Research Center (SAIC), Hampton, VA 23665